Biochimica et Biophysica Acta, 1151 (1993) 216–222

BBAMEM 76076

A near perfect temperature adaptation of bilayer order in vertebrate brain membranes

M.K. Behan-Martin [a], G.R. Jones [b], K. Bowler [c] and A.R. Cossins [a]

[a] *Environmental Physiology Research Group, Department of Environmental and Evolutionary Biology, University of Liverpool, Liverpool (UK),* [b] *Biology Support Laboratory, SERC Laboratory, Daresbury, Warrington (UK) and* [c] *Department of Biological Sciences, University of Durham, Durham (UK)*

(Received 9 March 1993)

Key words: Temperature adaptation; Bilayer order; Fluorescence anisotropy; DPH; *trans*-Parinaric acid; Time-resolved fluorescence; (Vertebrate brain membrane)

The bilayer order of a brain synaptic membrane fraction from a number of fish, mammalian and avian species have been compared in relation to their respective body temperatures using steady-state and time-resolved fluorescence anisotropy techniques. Fluorescence anisotropy for both 1,6-diphenyl-1,3,5-hexatriene and *trans*-parinaric acid increased in the order: antarctic *Notothenia*, trout, perch, cichlid, rat and starling, this also being the order of increasing body temperature. This suggests that cold-adapted fish species possess more disordered brain membranes than warm-adapted fish species, and mammals and birds membranes were more ordered than fish membranes. Comparison of temperature profiles for both fluorescence probes showed that fish species display similar anisotropies, and by inference bilayer order, to mammals and birds when measured at their respective body temperatures. Time-resolved analysis showed that the interspecific differences in $\langle P_2 \rangle$ order parameter was consistently related to body temperature whilst the rotational diffusion coefficient was not. These results suggest that brain membrane order is highly conserved within the vertebrates despite large differences in thermal habits and phylogenetic position. Polar fish species have by far the lowest bilayer order indicating that invasion of extreme cold habitats involved an adaptive decrease in bilayer order and conversely adoption of a high body temperature by mammals involved an adaptive increase in bilayer order. The conservation of membrane static order for these species at their respective body temperatures indicates a regulatory control of this aspect of membrane hydrocarbon structure and the functional importance of this structure.

Introduction

Membrane 'fluidity' or bilayer order has a major influence over a wide variety of membrane functions and processes [1]. This is because the motional properties and semi-ordered state of the hydrocarbon interior define and to some extent limit the conformational flexibility of membrane-bound proteins [2]. Given this importance it is reasonable to expect that lipid order is highly regulated. Perhaps the most convincing demonstrations of the adaptive regulation of membrane lipid order comes from studies on poikilothermic organisms such as microorganisms, protozoa, and fish following a change in the temperature of their surroundings [3]. A large number of studies have documented the decrease in bilayer order and increased unsaturation of membranes isolated from organisms following a reduction in temperature [4]. The change in order is commonly found to offset approx. 33–50% of the increase in order due to the direct effects of cooling [3].

Living organisms have evolved in a far wider range of thermal habitats than can be accommodated by any one species and it is commonly believed that membrane adaptations play a major role in genotypic as well as phenotypic environmental adaptation. However, the evidence for this is limited to the comparison of lipid composition in membranes of mammal and fish species [5] and only one study has compared physical structures of these membranes [6]. This showed a limited and unquantified degree of temperature compensation of brain synaptosomal membranes between a polar fish species and cold-acclimated goldfish and between a fish species which inhabits a warm desert spring and rat.

To examine more comprehensively the role of membrane bilayer order in the evolutionary adaptation of animals to temperature we have prepared a more refined brain membrane fraction from a wider range of

Correspondence to: A. Cossins, Environmental Physiology Research Group, Department of Environmental and Evolutionary Biology, University of Liverpool, PO Box 147, Liverpool L69 3BX, UK.

fish species from diverse thermal habitats and compared these with corresponding fractions from several species of birds and mammal. This membrane fraction is enriched in $(Na^+ + K^+)$-ATPase and is therefore considered to be derived largely from synaptic membranes. Central synapses are specifically thought to be amongst the most important sites of damage during exposure to altered high and low temperature [7] and hence provide a critical site for compensatory adaptation both over the evolutionary, as well as the seasonal timescales.

Materials and Methods

Animals

Species include: rat (*Rattus rattus*), mouse (*Mus musculus*), gerbil (*Gerbillus* sp.), hamster (*Mesocricetus auratus*), feral pigeon (*Columbia livia*), starling (*Sturnus vulgaris*), carp (*Cyprinus carpio*), goldfish (*Carassius auratus*), convict cichlid (*Cichlasoma nigrofaciatum*), perch (*Perca fluviatilis*), rainbow trout (*Onchorhynchus mykiss*) and the antarctic *Notothenia neglecta*. *N. neglecta* were obtained from the British Antarctic Survey, perch from a local canal, trout, carp and goldfish from commercial sources and cichlids were maintained as a culture. The birds were trapped wild and used immediately. All fish species were maintained in freshwater or seawater (*N. neglecta*) for not less than 21 days at different temperatures specified in Figs. 1 and 2.

Brain synaptic membranes

Brain membrane fractions were prepared by modifications of the procedure described earlier [8–10]. Membrane fractions were prepared from whole brain and were of synaptosomal origin as judged from marker enzyme activity and inspection by electron microscopy [8,11]. The crude synaptosomal fraction was pelleted by centrifugation at $11\,500 \times g$ for 20 min, and submitted to osmotic shock by homogenisation in 10 mmol l^{-1} imidazole (pH 7.2), 1 mmol l^{-1} EDTA. This lysed the synaptosomes releasing mitochondria and synaptic vesicles [8]. The lysate was centrifuged at $20\,000 \times g$ for 30 min and the pellet rehomogenised in 3 ml 10 mmol l^{-1} imidazole (pH 7.2), layered over a discontinuous sucrose gradient consisting of equal volumes of 0.8, 0.9, 1.0, 1.2 mol l^{-1} sucrose in 20 mmol l^{-1} imidazole (pH 7.2) and centrifuged at $100\,000 \times g$ for 2 h at 4°C. The membranes at the 0.9/1.0 interface for fish and 1.0/1.2 interface for mammals and birds were collected and the sucrose diluted to 0.8 mol l^{-1} with imidazole/EDTA buffer and sedimented at $100\,000 \times g$ for 60 min. The pellets were resuspended in a small volume of 10 mmol l^{-1} imidazole (pH 7.2) and used immediately or stored frozen at −20°C.

Assay of $(Na^+ + K^+)$-ATPase specific activity indicated an enrichment of synaptic membranes of 7-fold over the tissue homogenate. Marker enzymes for endoplasmic reticulum (NADPH : cytochrome-*c* reductase) and mitochondria (succinate dehydrogenase) were undetectable. We conclude that these membrane fractions are enriched in synaptic endings and had negligible mitochondrial contamination [8,10].

Steady-state fluorescence anisotropy

Membrane hydrocarbon order was estimated by measuring the fluorescence anisotropy of the membrane probes 1,6-diphenyl-1,3,5-hexatriene (DPH) and

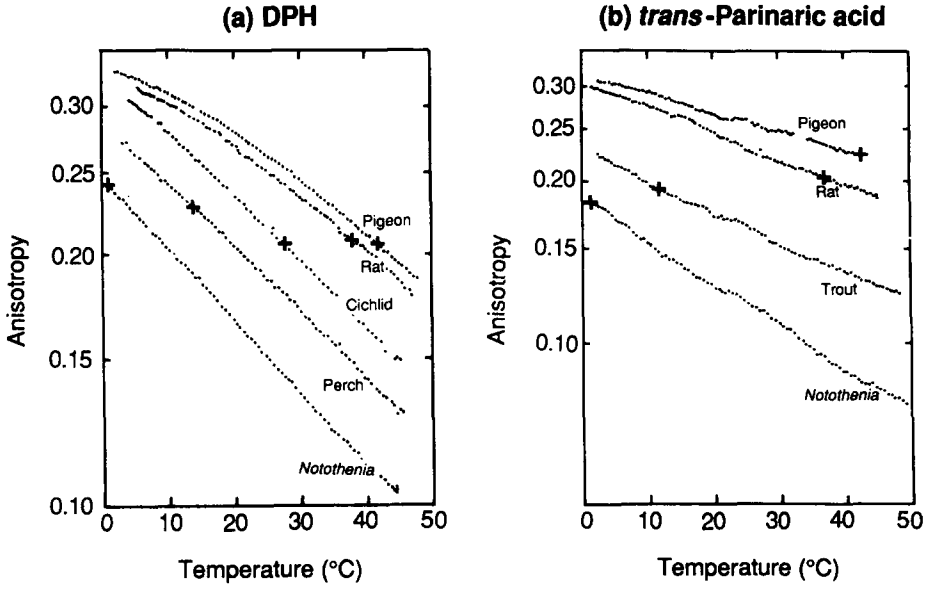

Fig. 1. Typical temperature profiles of anisotropy of DPH (a) and *trans*-parinaric acid (b) in brain membranes of fish, mammals and bird species. Values were determined during warming scans (0.75 C°/min). The crosses indicate the anisotropy at the acclimation or body temperature for each species.

trans-parinaric acid under steady illumination using the instrument described previously [12]. *trans*-Parinaric acid was used throughout under an atmosphere of oxygen-free nitrogen at a final concentration of $2.0 \cdot 10^{-6}$ mol l^{-1} and illumination was minimized.

Time-resolved anisotropy

This was determined as described previously [13] on the time-resolved port (HA12) of the Synchroton Radiation Source, Daresbury, Warrington, UK. The decay of fluorescence intensity was fitted with a triexponential decay law to Chi-squared values of 1.3 or less. Residual anisotropies were determined from a decay law incorporating a biexponential decay of anisotropy together with a residual anisotropy (r_∞). The $\langle P_2 \rangle$ order parameter is related to the time-resolved r_∞ by

$$r_\infty / r_0 = \langle P_2 \rangle^2$$

where r_0 is the limiting anisotropy. It is a more direct measure of membrane structural order [14]. Expressing order in this form accounts for changes in r_0 which can render the r_∞ term ambiguous. The rotational diffusion coefficient (D_{perp}) was calculated according to Ameloot et al. [14] by an extension of the simpler model-independent interpolation of Lipari and Szabo [15]. For stick-like probes with almost colinear absorption and emission dipoles, such as DPH and *trans*-parinaric acid, D_{perp} refers to rotation around an axis perpendicular to the symmetry axis of the molecule. For this purpose a short lifetime scattering component was extracted from the decay curves before analysis [13].

Results

DPH

Fig. 1a shows representative semilog temperature profiles for fluorescence anisotropy of DPH under steady illumination. The profiles for fish were linear and occured over a lower range of anisotropies than the curvilinear profiles of mammals and birds. The profiles for the fish species were clearly displaced with respect to each other with anisotropies increasing in the order *Notothenia* (0°C), perch (15°C) and cichlid (28°C) where the brackets indicate the temperatures to which the fish were exposed and acclimated before the experiment. Moreover, the profiles for the fish species were all substantially lower than for the mammalian and avian species.

The crosses in Fig. 1a show the anisotropy for each species at its respective acclimation (fish) or body (birds, mammals) temperature. It is clear that despite the large temperature dependence of DPH anisotropy that the anisotropies measured at in vivo temperatures for each of the different species were similar. It is remarkable that this relationship includes the homeothermic

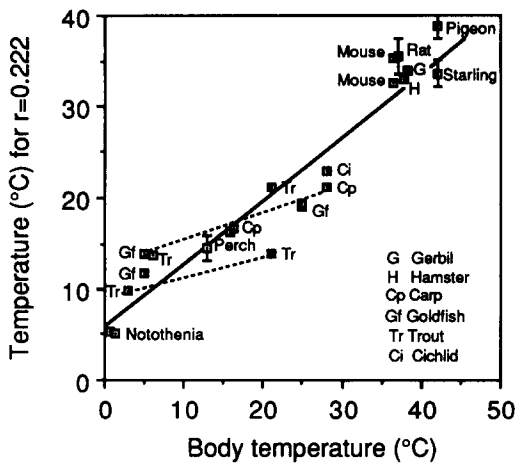

Fig. 2. The relationship between the temperature profile of DPH anisotropy and body temperature of fish, mammal and bird species. The position of the DPH anisotropy/temperature plot on the temperature axis was arbitrarily defined as the temperature for a given anisotropy (0.222) and this was plotted against the acclimation or body temperature for each species. Species include: rat (*Rattus rattus*), mouse (*Mus musculus*), gerbil (*Gerbillus* sp.), hamster (*Mesocricetus auratus*), pigeon (*Columbia livia*), starling (*Sturnus vulgaris*), carp (*Cyprinus carpio*), goldfish (*Carassius auratus*), cichlid (*Cichlasoma nigrofaciatum*), perch (*Perca fluviatilis*), rainbow trout (*Onchorhynchus mykiss*) and the antarctic *Notothenia neglecta*. The error bars represent ±S.E. for six (rat) or three (starling, pigeon, perch) preparations. For trout, carp and goldfish the symbols represent individual values for cold- and warm-acclimated groups of fish (4 weeks acclimation). The body temperatures for the mammals have been offset slightly for clarity. The solid line has been calculated by linear regression of all data points shown and thus represents interspecific or evolutionary adaptation. The upper dashed line connects values for both carp and goldfish acclimated to different temperatures and the lower dashed line connects values for one preparation each from cold-and warm-acclimated trout (see Results). These lines represent the shift in temperature profiles caused by phenotypic as opposed to genotypic adaptation.

birds and mammals to the extent that the anisotropy for the antarctic fish at 0°C was not greatly different from that of the rat at 37°C.

The magnitude of the interspecific differences in relation to the temperature dependence of anisotropy can be more readily assessed by reference to Fig. 2. Here we have determined from the temperature profiles the assay temperature for which DPH anisotropy was at a set arbitrary value and plotted this against body temperature for 12 species. This procedure indicates the difference in the position of the anisotropy profiles on the temperature axis so that if all species displayed identical temperature profiles the resulting graph would have a slope of zero whilst if the profiles provided identical anisotropies at their respective body temperatures the slope in Fig. 2 would be 1. The line which passes through all fish, bird and mammal points has a least-squares slope of 0.70 which indicates that the interspecific differences in anisotropy compensate for 70% of the direct effects of temperature. The

reference anisotropy was 0.222, this value being midway between the anisotropies at the respective body temperature for *Notothenia* and rat. Choosing a different reference anisotropy does not affect this conclusion.

Fig. 2 also includes data for goldfish, carp and trout which had been acclimated to cold or warm for several weeks. The dashed lines connecting the data points for cold- and warm-acclimated carp and goldfish showed a slope of approx. 0.35. The first pair of cold- and warm-acclimated membrane preparations for trout also showed a slope of approx. 0.35, though a second pair of preparations produced values which corresponded more closely with the dashed line for carp and goldfish. The two trout data sets were produced at different times of the year and may represent a seasonal variation which is independent of temperature.

trans-Parinaric acid

One problem of interpretation comes from uncertainty regarding the precise positional distribution of DPH in brain membranes. *trans*-Parinaric acid more closely resembles the structure of the acyl groups of the hydrocarbon interior than does DPH and, by virtue of its charged headgroup, has one pole securely located close to the headgroup region of the membrane. We have therefore compared the membranes from *Notothenia*, trout and rat using this probe (Fig. 1b). Steady-state anisotropy profiles displayed the same large interspecific differences as DPH with broadly similar anisotropies for each species at their respective in vivo body temperature. Plotting these four profiles according to the procedure shown in Fig. 2 produced a slope somewhat in excess of unity.

Time-resolved studies

Fig. 3 compares the $\langle P_2 \rangle$ order parameter for *Notothenia*, trout and rat using both DPH and *trans*-parinaric acid. The interspecific differences in order parameter closely matches those observed with steady-state anisotropy. Fig. 4 shows the corresponding rotational diffusion coefficients. Whilst there were differences between species they did not correspond with differences in body temperatures. Moreover the interspecific differences varied between the two membrane probes. The rat membranes consistently displayed the lowest rotational diffusion coefficients with both probes but with DPH *Notothenia* displayed the greatest values and with *trans*-parinaric acid trout displayed the greatest values.

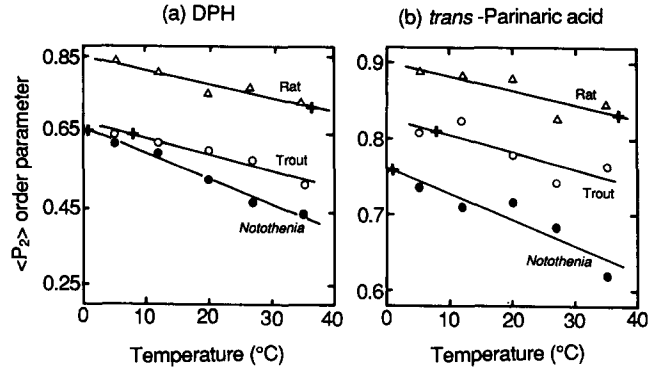

Fig. 3. $\langle P_2 \rangle$ order parameters for for single preparations of synaptic membranes from *N. neglecta*, trout and rat using either (a) DPH and (b) *trans*-parinaric acid as membrane probe. Again the crosses indicate the $\langle P_2 \rangle$ order parameter at the acclimation or body temperature for each species.

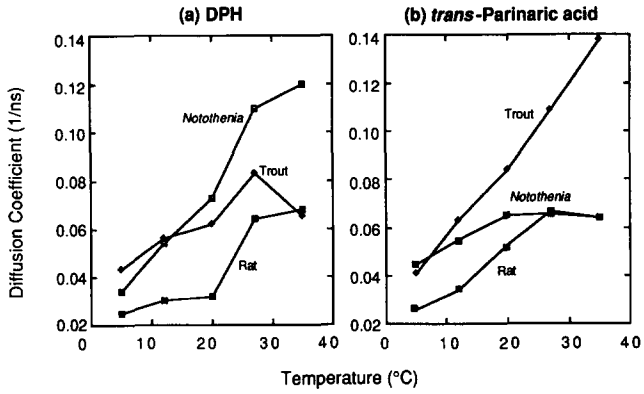

Fig. 4. The rotational diffusion coefficient for for single preparations of synaptic membranes from *N. neglecta*, trout and rat using (a) DPH and (b) *trans*-parinaric acid as membrane probe. Values were calculated directly from the decay curves.

Discussion

A previous comparison of a polar fish species with 5°C acclimated goldfish showed a compensation of bilayer order of the arctic species to extreme cold [6]. Similarly the corresponding membrane fraction from rat was more ordered than that from warm acclimated goldfish and the desert pupfish which was taken as evidence of a compensation of rat membranes to their high body temperature. However, in neither case were the DPH anisotropies measured at their respective body temperatures identical. The work described here extends these basic observations firstly by using a more refined membrane fraction, secondly by using a greatly increased number of species we develop a more quantitative relationship between adaptation temperature and bilayer order and, thirdly, by extending the analysis of membrane physical structure into the time-resolved domain.

The steady-state experiments demonstrate large differences between fish species in bilayer order with a clear and orderly correlation between bilayer physical structure and the body temperature normally experienced by each species. Thus, the order of increasing

anisotropy (and by inference bilayer order) was *N. neglecta*, trout, perch, carp = goldfish and the East African *C. nigrofasciatum* and this exactly matches the order of increasing adaptation temperature. The mammalian and avian species displayed DPH anisotropies which were similar to each other and which corresponded to their similar body temperatures. These anisotropies were substantially greater than those recorded for the fish species which corresponds to their much higher body temperatures.

These observations indicate that the relationship between body temperature and bilayer order, at least as indicated by DPH anisotropy, crosses broad phylogenetic boundaries to include the homeothermic mammals and birds. The generality of this relationship within the vertebrates is illustrated by a single line in Fig. 2 which apparently connects all species, irrespective of phylogenetic position. This method of presentation emphasizes the interspecific differences in membrane structure by reference to the position of the anisotropy/temperature curves on the temperature axis. This is plotted as a function of adaptation temperature and the resulting slope matches the previously described method for calculating homeoviscous efficacy, this being a measure of the temperature compensation achieved. The slope of this line calculated statistically was 0.70. In that this slope would display a slope of unity if each species possessed an identical anisotropy at their respective body temperatures our results suggest that the interspecific differences in membrane structure was sufficient to overcome approximately three quarters of the direct effects of temperature upon membrane structure; thus homeoviscous efficacy or HE was 70% [3]. This represents a substantial homeoviscous adaptation over the evolutionary timescale which contrasts with the smaller adaptations reported for synaptic membranes of fish acclimated for several weeks to different temperatures (Ref. 3, 30–50%). The principal exceptions to this statement are the basolateral membranes of fish intestinal mucosa which may display HE values of 60–75% [16,17] and the lack of homeoviscous adaptation in muscle sarcoplasmic reticulum [18] and the intestinal brush border [16].

There is some uncertainty regarding the precise positional distribution of DPH within the depth profile of the bilayer [19] and this leads to uncertainty regarding the exact significance of anisotropy measurements to bilayer structure. However, this is not true of *trans*-parinaric acid because not only does this probe resemble the fatty acid structure more closely but its charged headgroup is located close to the headgroup region of the bilayer so that the hydrocarbon chain reports on conditions at a specified depth in the depth gradient of acyl group segmental mobility [19]. We show here that this probe displays similar if not identical interspecific differences in steady-state anisotropy to that shown by DPH. It seems reasonable therefore to discount artifactual effects due to variations in the positional distribution of DPH and to conclude that the interspecific differences result from differences in probe rotational characteristics caused by differences in membrane structural order. At this point it is worth noting that the interspecific differences observed using *trans*-parinaric acid were somewhat greater than for DPH suggesting that HE might approach or slightly exceed 100% depending upon the precise technique or probe used to define 'fluidity' or order. This difference in HE for the two probes is probably caused by differences in their binding distributions and rotational characteristics, especially the tethered nature of *trans*-parinaric acid motion. However, the broad agreement in the magnitude and direction of the interspecific differences with two probes of quite distinct binding distributions and different fluorescence characteristics strengthens the conclusion of large, possibly complete, thermal compensations of lipid order in vertebrate brain membranes.

Steady-state anisotropy of rod-shaped fluorescence probes such as DPH is a function of two parameters, namely the orientational order of the probes environment and the rate of probe rotational motion [20]. Measuring the time dependence of emission anisotropy after pulsed excitation provides a direct means of distinguishing between the two and separating their role in membrane adaptation [14,21]. We have therefore analysed the time-resolved decays of DPH anisotropy using synchrotron radiation to determine the rotational diffusion coefficient, a measure of the wobbling diffusion rate of the probe, and the $\langle P_2 \rangle$ order parameter, a measure of the degree of local hydrocarbon ordering.

The rotational diffusion coefficient showed inconsistent interspecific trends and this corresponds with the absence of differences between membranes of temperature-acclimated goldfish in studies using differential polarised phase measurements [22]. At this point it is worth pointing out that these more recent time-resolved experiments in which the rotational diffusion coefficient was measured directly from the decay curve should be distinguished from earlier studies [23] which showed adaptations of a 'rotational diffusion coefficient'. This latter parameter was calculated from steady-state polarization measurements using the Perrin equation. This equation assumes isotropic and unhindered rotational motion of the probe, a condition which for some time has been recognised as being inappropriate for both DPH and *trans*-parinaric acid in biological membranes [20,21]. It is emphasised that because the intraspecific differences in the earlier studies have their origin in differences in polarisation they are entirely consistent with both the steady-state and the time-resolved studies presented here.

In contrast to the rotational diffusion coefficient, the $\langle P_2 \rangle$ order parameter shows differences between *N. neglecta*, trout and rat which correspond with those observed using the steady-state technique. With DPH there was an almost perfect compensation between the membranes of *Notothenia* and trout whilst those of rat showed an overcompensation relative to trout. Conversely, with *trans*-parinaric acid there was considerable overcompensation between *Notothenia* and trout but perfect compensation between trout and rat. Again these minor difference between the probes is ascribed to differences in binding distributions and rotational characteristics. However, it is clear that HE for the time-resolved $\langle P_2 \rangle$ order parameter was consistently greater than the steady-state anisotropy for both probes. The lower HE of the steady-state method may be due to a small but significant influence of the rate of rotational motion of the probe upon the observed anisotropy [24]. In that there was no consistent difference between species in the rotational diffusion coefficient, this influence would reduce the differences between species in anisotropy. These observations support two conclusions: firstly the simpler steady-state method consistently underestimates HE relative to the compensation observed in the more rigorous time-resolved domain and secondly it is those features of membrane structure which influence the amplitude of probe wobbling motion, rather than its reorientational rate, which are under adaptive, regulatory control. This change in the microenvironmental hindrance to probe motion is taken as evidence of an adjustment to the orientational order of the hydrocarbon chains of the membrane interior by means of altered lipid composition. One reason why the rotational diffusion coefficient does not display consistent interspecific differences is that it is sensitive to fast reorientational motion of the probe within its local hydrocarbon microenvironment and this motion may be susceptible to the local perturbation by the probe itself. The extent of probe rotation, which largely defines the r_∞, is not so affected by probe disruption of the microenvironment.

In summary, both the steady-state and the time-resolved analysis shows that there are substantial differences in the acyl chain order of brain membranes of different vertebrate species. These differences correlate both in direction and magnitude with body temperature, such that when anisotropy is determined at their respective body temperatures all species show broadly similar if not identical values. This suggests that the differences between species are linked to and compensate for differences in the temperature of their tissues. Thus the evolutionary invasion of extreme cold habitats involves an adaptive decrease in order to offset the cold-induced ordering and vice verse. This is mechanistically related to at least one of several potential lipid adaptations, namely the proportion of unsaturated lipids [25–27]. Whilst the nature and precise functional significance of the conserved membrane order remains ill-defined [28.29], its preservation in such a wide range of vertebrate species offers strong support for its adaptive importance. The large compensatory responses in animals from different thermal habitats to which they have become genotypically adapted contrasts with the rather smaller adaptations observed during acclimation of individuals to altered temperature. It seems that in this, as in other respects, the potentialities of evolutionary adaptation far outstrips the physiological ability of any one species to acclimatise.

Acknowledgements

We thank Ms J. Bridson for skilled technical assistance, S.E.R.C. for beamtime on the synchrotron radiation source and the British Antarctic Survey for living specimens of *Notothenia* sp.

References

1 Shinitzky, M. (1984) in Physiology of Membrane Fluidity (Shinitzky, M., ed.), Vol. 1, pp. 1–53, CRC Press, Boca Raton.
2 Deuticke, B. and Haest, C.W.M. (1987) Annu. Rev. Physiol. 49, 221.
3 Cossins, A.R. and Sinensky, M. (1984) Physiology of Membrane Fluidity (Shinitzky, M., ed.), Vol. 2, pp. 1–20, CRC Press, Boca Raton.
4 Hazel, J.R. and Williams, E. (1990) Prog. Lipid Res. 29, 167–227.
5 Hazel, J.R. and Prosser, C.L. (1972) Physiol. Rev. 54, 620–677.
6 Cossins, A.R. and Prosser, C.L. (1978) Proc. Natl. Acad. Sci. USA 75, 2040–2043.
7 Cossins, A.R., Friedlander, M.J. and Prosser, C.L. (1977) J. Comp. Physiol. 120, 109–121.
8 Rodriguez de Lores Arnaiz, G., Alberici, M. and de Robertis, E. (1967) J. Neurochem. 14, 215–225.
9 Bowler, K. and Tirri, R. (1976) J. Neurochem. 23, 611.
10 Cossins, A.R. and Prosser, C.L. (1982) Biochim. Biophys. Acta 687, 303–309.
11 Lewis, R.N.A.H. (1978) Ph.D. Thesis, University of Durham.
12 Cossins, A.R. and Macdonald, A.G. (1986) Biochim. Biophys. Acta 860, 325–335.
13 Behan-Martin, M.K., Macdonald, A.G., Jones, G.R. and Cossins, A.R. (1992) Biochim. Biophys. Acta 1103, 317–323.
14 Ameloot, M., Hendrickx, H., Herreman, W., Pottel, H., Van Cauwelaert, F. and Van der Meer, W. (1984) Biophys. J. 46, 525–539.
15 Lipari, G. and Szabo, A. (1980) Biophys. J. 30, 489–506.
16 Lee, J.A.C and Cossins, A.R. (1990) Biochim. Biophys. Acta 1026, 195–203.
17 Scharzbaum, P.J., Wieser, W. and Cossins, A.R. (1991) Physiol. Zool. 65, 17–34.
18 Cossins, A.R., Christiansen, J. and Prosser, C.L. (1978) Biochim. Biophys. Acta 511, 442–454.
19 Wolber, P.K. and Hudson, B.S.(1981) Biochemistry 20, 2800.
20 Van der Meer, W. (1984) in Physiology of Membrane Fluidity (Shinitzky, M., ed.), Vol. 1, pp. 53–72, CRC Press, Boca Raton.
21 Van der Meer, W., Pottel, H., Herreman, W., Ameloot, M. and Hendrickx, H. (1984) Biophys. J. 46, 515–525.

22 Cossins, A.R., Kent, J. and Prosser, C.L. (1980) Biochim. Biophys. Acta 599, 341–358.
23 Cossins, A.R. (1977) Biochim. Biophys. Acta 470, 395–411.
24 Van Blitterwijk, W.J., Van Hoeven, R.P. and Van der Meer, B.W. (1981) Biochim. Biophys. Acta 644, 323–332.
25 Hazel, J.R. (1988) Advances in Membrane Fluidity (Aloia, R.C., ed.), pp. 149–188, Alan R. Liss, New York.
26 Cossins, A.R. and Macdonald, A.G. (1989) J. Bioeng. Biomembr. 21, 115–135.
27 Behan, M. (1989) Ph.D. Thesis, University of Liverpool.
28 Macdonald, A.G. (1988) Biochem. J. 256, 313–327.
29 Macdonald, A.G. (1990) Biochim. Biophys. Acta 1031, 291–310.